RAPID COMMUNICATIONS

PHYSICAL REVIEW B VOLUME 34, NUMBER 8 15 OCTOBER 1986

Optical bowing in zinc chalcogenide semiconductor alloys

James E. Bernard and Alex Zunger
Solar Energy Research Institute, Golden, Colorado, 80401
(Received 9 June 1986)

Alloys of zinc chalcogenides exhibit both some of the smallest (for ZnS_xSe_{1-x}) and the largest (for ZnS_xTe_{1-x}) optical bowing observed in isovalent semiconductor systems. A theoretical analysis of this effect, by use of self-consistent band-structure techniques for ordered 50%-50% alloys in the CuAu-I structure, predicts correct bowing parameters and chemical trends, yet suggests a physical model which is altogether different from the virtual-crystal model.

The smooth variation with composition x of the lattice parameter $a(x)$ and the optical band gap $E_g(x)$ of isostructural, isovalent semiconductor alloys[1] $A_xB_{1-x}C$ has long formed the basis for their extensive utilization in semiconductor technologies, which often require a's and E_g's intermediate between those of pure binary compounds AC and BC. Whereas $a(x)$ often can be estimated accurately from a *linear* interpolation[1] $a(x) \cong xa_{AC} + (1-x)a_{BC}$ between the lattice parameters a_{AC} and a_{BC} of the constituents (Végard's rule), the optical band gaps of alloys show quadratic nonlinearities.[1,2]

$$E_g(x) = [x\varepsilon_{AC} + (1-x)\varepsilon_{BC}] - bx(1-x) \ . \qquad (1)$$

Perhaps the most striking example of this "optical bowing" effect ($b \neq 0$) is offered by solid solutions of zinc chalcogenides,[2-5] exhibiting (Table I) both one of the smallest bowing parameters ($b \cong 0^2$–0.4^3 eV for ZnS_xSe_{1-x}) and the largest ($b \cong 3$ eV in[5] ZnS_xTe_{1-x}) ever to be observed in isovalent pseudobinary semiconductor alloys.

Current understanding of the origin of the experimental (expt) optical bowing parameters rests[6-9] on a separation of b_{expt} into a contribution b_I present in an ideal hypothetical alloy (either perfectly substitutionally random or perfectly ordered), modeled within the virtual-crystal approximation (VCA), and a contribution b_{II} due to alloy disorder.[7(a),9] In VCA models of an $A_xB_{1-x}C$ alloy[6-9] the atoms A and B are replaced by some average atom $\langle AB \rangle$ whose properties are modeled as a linear average of those of A and B. Hence, unlike a true *ternary* system, the $\langle AB \rangle C$ *virtual* alloy is assumed to have the following: (i) a single type of nearest-neighbor bond with length $R_{\langle AB \rangle C}$, (ii) the crystal structure common to AC and BC, and concomitantly, (iii) a *linearly* averaged crystal potential (and crystal screening); hence symmetries of the band structure and charge densities identical to those of the underlying binaries. These assumptions constitute an enormous computational simplification, for the alloy band structure can be treated precisely with the same computational tools used to describe each of its binary constituents. This simplicity is largely responsible for the great popularity this approach has enjoyed over the years[6-9] within diverse computational schemes such as the empirical pseudopotential method,[6,7] the dielectric two-band model,[6] and tight binding.[8,9]

Recent experimental[10-12] and theoretical[13] studies have been critical of the VCA, demonstrating that assumptions (i)–(iii) above are inappropriate to an accurate model of semiconductor alloys. These studies have found (i) bimodal ($R_{AC} \neq R_{BC}$) bond-length distributions,[10,13] (ii) lower symmetry (partially ordered) alloy space groups with distinct A and B sublattices,[13,14] and (iii) the identification of distinct $A-C$ and $B-C$ features in the alloy photoemission,[11(a)] reflectivity,[11(b)] and nuclear magnetic resonance chemical shift spectra.[12] In addition, the wide range of degrees of success[5-9] enjoyed by VCA-based approaches to the optical bowing problem (depending on the method used to interpolate the band parameters of the alloy from those of the constituents) reduces one's confidence in the VCA itself. In cases where the VCA contribution b_I^{VCA} fell substantially short of the experimental value b_{expt}, the remainder was ascribed to disorder effects.[5,6] However, such large disorder contributions appear to be inconsistent with experimental evidence in the case of size-mismatched alloys, which show remarkably sharp Raman lines, sharp reflectivity spectra,[4,11(b)] high electron mobilities,[1] etc., and with coherent potential calculations,[11(a)] which show little additional bowing (b_{II}) due to disorder.

For these reasons, we approach the optical bowing problem from an altogether different viewpoint, using a nonempirical, self-consistent approach free of the VCA and motivated as follows. Alloys can be described as collections of local atomic arrangements (clusters), each of which occurs with a statistical weight appropriate to the composition.[13,15] These same local arrangements occur in

TABLE I. Observed (Refs. 2–5) and calculated bowing parameters (in eV) of the fundamental direct band gap in zinc chalcogenide alloys. The observed lattice parameters a = 5.409, 5.668, and 6.089 Å were used for ZnS, ZnSe, and ZnTe, respectively. The calculated u_{eq} are 0.236, 0.229, and 0.215 for Zn_2SSe, Zn_2SeTe, and Zn_2STe, respectively.

Alloy	b_I^{VCA}	b_{expt}	b_I^{calc}	b_S	b_{CE}	b_{VD}
ZnSSe	0.14[a]	0.43[b]	0.39	0.45	0.03	−0.09
ZnSeTe	−0.04[a]	1.23[c]	1.96	1.32	1.00	−0.36
ZnSTe	0.28[a]	~3.0[d]	3.83	2.68	1.68	−0.53

[a]Reference 6.
[b]Reference 3.
[c]Reference 4.
[d]References 2 and 5.

nearest-neighbor clusters of four A and B atoms lying at the vertices of a tetrahedron, are A_4, A_3B, A_2B_2, AB_3, and B_4 which occur also in the ordered phases AC, A_3BC_4, ABC_2, AB_3C_4, and BC, respectively. Since zinc chalcogenide alloys exhibit the face centered cubic (fcc) structure for all compositions,[2-5] a superposition of these five structures $A_nB_{4-n}C_4$ for $0 \le n \le 4$ (all fcc sublattices) correctly describes the Bravais lattice of the alloy.[13] We consider *equilibrium* structures by allowing the common atom C (in our case Zn) to relax to its minimum energy position (generally producing nonequal $A-C$ and $B-C$ bond lengths[10,13]) for each structure n at its appropriate equilibrium lattice constant $a^{(n)}$. We limit further the number of structures to be considered to AC, ABC_2, and BC by noting that (i) the bowing b does not depend on composition x to a very good approximation [Eq. (1)], hence one can select any value of x, (ii) choosing $x=\frac{1}{2}$, the ABC_2 structure occurs with overwhelmingly larger concentration than A_3BC_4 and AB_3C_4 at this composition.[13] Hence we neglect any shift in the band gap contributed by *minority* species at $x=\frac{1}{2}$ (i.e., disorder effects).

Among the benefits of this approach are the following: (i) the calculation can be done by a first-principles method (unlike VCA which requires a potential averaging which is not amenable to a first-principles description), (ii) the unique identities of the A and B atoms are retained (hence A-B charge transfer is permitted), and (iii) distinct bond lengths R_{AC} and R_{BC} are permitted. The reasonable agreement obtained with experiment (Table I) implies the relative unimportance of disorder effects for these size-mismatched alloys, contrary to previous conclusions,[6] suggests a physical origin of bowing effects completely different from that implied by the VCA, and indicates a crucial experiment which can distinguish clearly the validity of the two approaches.

We use the first-principles self-consistent all-electron mixed-basis band-structure method[16] within the local-density formalism. Convergence tests[16] have assured a precision of ~ 0.1 eV or better for band energies. We have used a simple tetragonal ABC_2 structure derived from that of the CuAu-I alloy[13,14] by the inclusion of an additional simple tetragonal sublattice occupied by a third type of atom (Zn here). It is characterized by the space group $P\bar{4}m2$, a tetragonal $\eta = c/a$ ratio (assumed unity, in accordance with the observed[2-5] cubic lattice parameters of the alloys), and an internal displacement parameter u measuring a possible difference between the two bond lengths $R_{AC}=(\eta^2u^2+\frac{1}{8})^{1/2}a$ and $R_{BC}=[\eta^2(u-\frac{1}{2})^2+\frac{1}{8}]^{1/2}a$. If $u=\frac{1}{4}$, then $R_{AC}=R_{BC}$, as in VCA. This structure has been observed previously[14] and used theoretically[13] for III-V alloys.

We follow the evolution of the bands of the ordered alloy model $A_nB_{4-n}C_4$ from those of its constituents AC and BC in three steps.[13] *First*, dilate the AC lattice and compress the BC lattice to a common lattice constant $a=a(x)$ appropriate to the alloy. This volume deformation (VD) contributes (for the 50%-50% alloy)

$$b_{\rm VD}=2[\varepsilon_{AC}(a_{AC})-\varepsilon_{AC}(a)]+2[\varepsilon_{BC}(a_{BC})-\varepsilon_{BC}(a)] \ ; \tag{2}$$

while it could be calculated from the known band gap deformation potentials of AC and BC, we calculate it directly from the volume-dependent band structures. *Second,* bring together n units of AC and $4-n$ units of BC, both with lattice constant $a(x)$, to form the compound alloy $A_nB_{4-n}C_4$, without relaxing the $A-C$ and $B-C$ bond lengths. The charge exchange (CE) between the units forming the alloy contributes (again for $n=2$)

$$b_{\rm CE}=2[\varepsilon_{AC}(a)+\varepsilon_{BC}(a)]-4\varepsilon_{ABC}(a,u=\tfrac{1}{4}) \ . \tag{3}$$

Third, allow the $A-C$ and $B-C$ bond lengths to relax to their equilibrium (eq) total energy minimizing value (hence, $u_{\rm eq}\neq\frac{1}{4}$). This structural ($S$) contribution is

$$b_S=4\varepsilon_{ABC}(a,u=\tfrac{1}{4})-4\varepsilon_{ABC}(a,u_{\rm eq}) \ . \tag{4}$$

All terms in Eqs. (2)-(4) are calculated separately via self-consistent band-structure calculations for the appropriate structues. The sum $b_{\rm I}=b_{\rm VD}+b_{\rm CE}+b_S$ of Eqs. (2)-(4) produces just the total bowing of Eq. (1) for $x=\frac{1}{2}$. Although we could have calculated this sum directly as $b_{\rm I}=2\varepsilon_{AC}(a_{AC})+2\varepsilon_{BC}(a_{BC})-4\varepsilon_{ABC}(a,u_{\rm eq})$ with just three band-structure calculations per alloy, we believe that the three-step process outlined above serves to clarify the physical origins of $b_{\rm I}$ in terms of (i) a hydrostatic pressure effect ($b_{\rm VD}$), (ii) a charge-transfer effect ($b_{\rm CE}$), and (iii) structural bond-length and bond-angle relaxation (b_S).

Equations (2)-(4) require the knowledge of the lattice constants a_{AC} and a_{BC} of the endpoint compounds (taken here from experiment, Table I), as well as $a(x)$ (from Végard's rule) and $u_{\rm eq}$ for the alloy at $x=\frac{1}{2}$. For the latter, we follow the method of Martins and Zunger,[17] who obtained alloy bond lengths in excellent agreement with experiment by minimizing the bond-bending and bond-stretching deformation energy, using Keating's valence force field.[18] Our results are summarized in Table I.

A few observations are apparent from the results. *First,* the calculated total bowing $b_{\rm I}^{\rm calc}$ reproduces well the observed values and their trends (the observed value of ZnS_xTe_{1-x} is the least certain since this sample was *metastably* grown[5] inside the miscibility gap). This leaves smaller discrepancies $b_{\rm expt}-b_{\rm I}^{\rm calc}$ to be accounted for by disorder contributions $b_{\rm II}$ relative to those suggested by the VCA[6] (compare $b_{\rm expt}-b_{\rm I}^{\rm VCA}$ in Table I). *Second,* the structural contribution b_S, neglected altogether in the VCA,[6-9] dominates $b_{\rm I}^{\rm calc}$. This is so because the band structure is extremely sensitive to bond deformations[19] (measured by $|u-\frac{1}{4}|$, where $u_{\rm eq}$ values are given in the caption of Table I), and since in turn, substantial bond deformations are required to relax the elastic strain energy[17] imposed by packing of binary components with a large lattice mismatch $\Delta a=|a_{AC}-a_{BC}|$ (hence, $b_S\propto\Delta a^2$). *Third,* the VD contributions are negative, since the increase in ε_{BC} due to compression of a_{BC} exceeds the decrease in ε_{AC} due to dilation of a_{AC}. *Fourth,* the CE contributions are positive, and as can be expected, increase monotonically with the electronegativity difference $\Delta\chi=|\chi_A-\chi_B|$ (0.1, 0.3, and 0.4, on Pauling's scale, for S-Se, Se-Te, and Te-S, respectively). The significance of the *dual* scaling with both Δa and $\Delta\chi$ is exemplified by the fact that $Ga_xAl_{1-x}As$ has a small bowing[7(a)] despite hav-

ing $\Delta\chi = 0.1$, just as does ZnS_xSe_{1-x}, which has a larger bowing $b \cong 0.5$ eV; the difference is traceable to the former alloy's having $\Delta a \cong 0$, while the latter has a substantial mismatch, $\Delta a = -0.26$ Å, giving it a significant contribution from b_S.

The departure from the VCA in these systems is evident most clearly in the calculated band-by-band charge densities depicted in Fig. 1. The two columns at the extreme left and extreme right depict, for ZnS and ZnTe, respectively, the calculated densities in the (110) plane, including those for the valence-band minimum (VB min) Γ_{1v} [Figs. 1(a) and 1(c)], the X_{1v} band [Figs. 1(d) and 1(f)], the valence-band maximum (VB max) Γ_{15v} [Figs. 1(g) and 1(i)], and the conduction-band minimum (CB min) Γ_{1c} [Figs. 1(j) and 1(l)]. As expected, the contours pertinent to the binary compounds are symmetric about the vertical plane containing the Zn site (dashed vertical lines in Fig. 1). Were the VCA description accurate, the contours for the ABC_2 alloy (center column of Fig. 1) would be symmetric too. This is obviously not the case: The VB min, $\Gamma_{1v}(\Gamma_{1v})$, of $STeZn_2$ [Fig. 1(b)] has a strong sulfur s-like character with little amplitude on Te; the next band, Γ_{1v} folded in from zinc blende X_{1v} is complementary in having most of its amplitude around Te [Fig. 1(e)]. Hence we predict a splitting of 2.6 eV between these two lowest valence bands at Γ to be obseved in photoemission (zero in VCA). A similar effect has been observed in photoemission in the valence band of $Hg_xCd_{1-x}Te$ alloys.[11(a)] In addition to the splitting due to folding, some states which would be degenerate due to folding alone (e.g., at M, de-

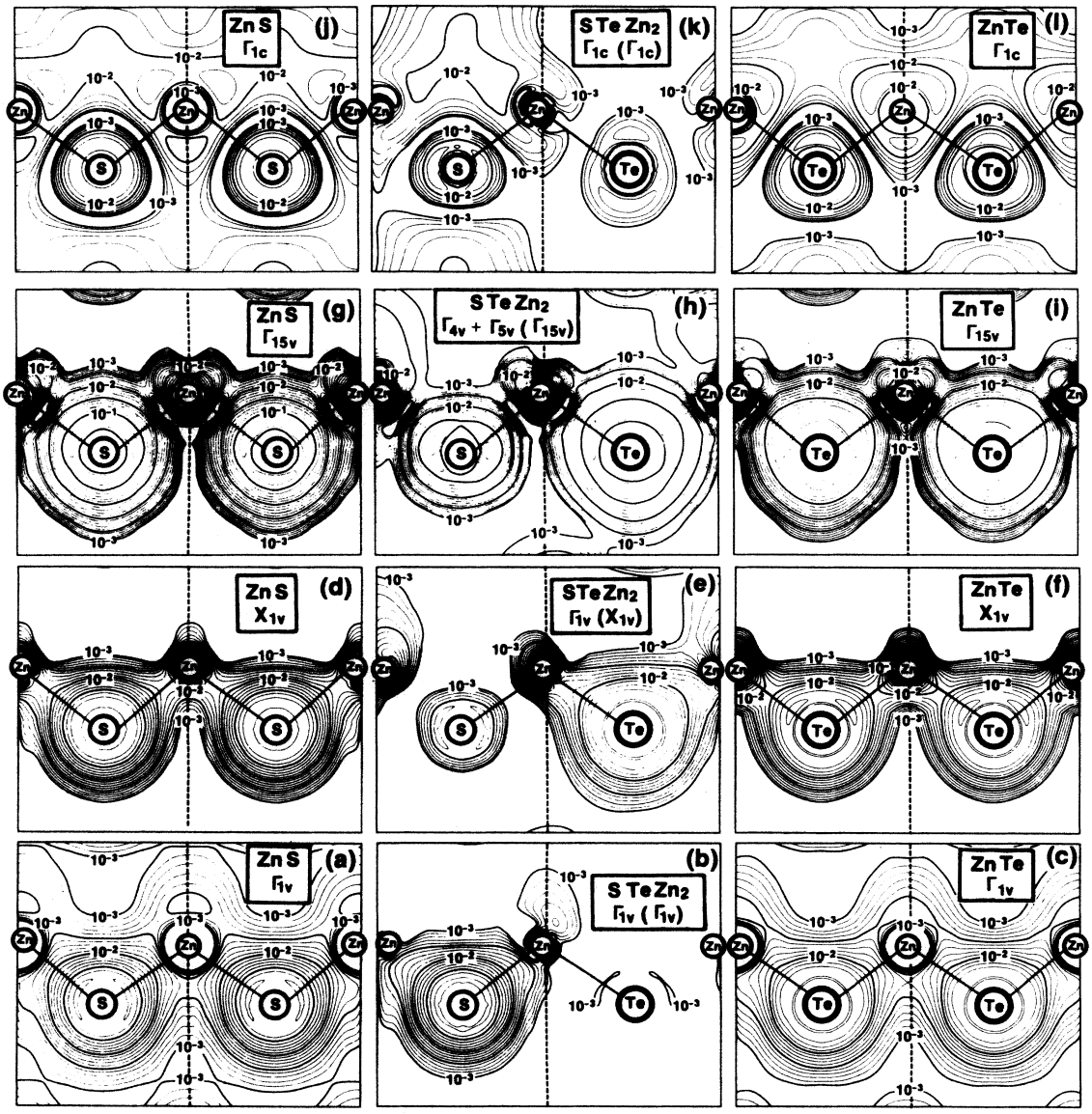

FIG. 1. Electronic charge-density contours (logarithmically spaced, in units of e/a.u.^{3}) of a few electronic states in ZnS (left), ZnTe (right), and their $STeZn_2$ alloy in the CuAu-I type structure (center). For the latter, we show both the band labels in $P\bar{4}m2$ symmetry and, in parentheses, the zinc-blende labels. Solid circles around atoms indicate core regions; straight solid lines denote bonds. The vertical dashed line is the symmetry plane for pure ZnS or ZnTe; this symmetry is broken in the alloy (central panels).

completely ordered structures. For example, the possible rived from two zinc-blende X points, and at R, derived from two zinc-blende L points) split in the alloy due to non-zinc-blende components of the potential. This splitting differs qualitatively in the case of mixed anions (e.g., Zn_2STe) from that in the case of mixed cations [e.g., $CdMnTe_2$ (Ref. 20) or $GaAlAs_2$]. For example, the lowest two valence states at M, being anion states, are split in the materials we consider here (with a splitting of 2.7 eV in Zn_2STe), whereas they are degenerate[20] in $CdMnTe_2$. The lowest two valence bands and lowest two conduction bands at R (all R_1) are split by 2.5 and 1.6 eV, respectively, in Zn_2STe. Similarly there are states which split in structures with mixed cations but are degenerate in the case of mixed anions. All such splittings must vanish in zinc blende (hence in VCA), which has neither mixed anions nor mixed cations, so photoemission measurements of these splittings would provide a critical test of the VCA *versus* the present physical model of bowing. Furthermore, in assuming the alloy to share with its constitutents the same space group symmetry, the VCA would predict the VB max, Γ_{15v}, to be a pure $p+d$ state [as in Figs. 1(g) and 1(i) for ZnS and ZnTe, respectively], and the CB min, Γ_{1c}, to be a pure s state [as in Figs. 1(j) and 1(l) for ZnS and ZnTe, respectively]. However, substantial intermixing of valence- ($\Gamma_{4v}+\Gamma_{5v}$) and conduction- (Γ_{1c}) band character is evident in our alloy calculation [Figs. 1(h) and 1(k)], this being precisely what is required to explain the observed bowing[21] of the spin-orbit splitting of the VB max. The significant departures from VCA noted in this and other work suggest a reexamination of applications of VCA to semiconductor alloys.

Note added in proof. Recently, J. C. Mikkelson and J. B. Boyce {paper presented at the *Seventh International Conference on Ternary and Multinary Compounds, Snowmass, Colorado, Sept. 1986,* edited by S. K. Deb and A. Zunger [Mater. Res. Soc. Symp. Proc. (to be published)]} have measured the Zn—Se and Ze—Te bond lengths in $ZnSe_xTe_{1-x}$ alloys using the extended x-ray absorption fine structure (EXAFS) method, finding at $x=0.5$ $R_{ZnSe}=2.472$ Å and $R_{ZnSe}=2.617$ Å, in excellent agreement with the values $R_{ZnSe}=2.472$ Å, and $R_{ZnTe}=2.616$ Å, calculated here from minimization of the elastic energies (corresponding to $u_{eq}=0.229$, caption to Table I).

This work was supported by Office of Energy Research-Basic Energy Sciences through Materials Research Division, Grant No. DE-AC02-77-CH00178. One of us (J.E.B.) wishes to thank J. Jaffe for consultations regarding the use of the "potential-variation-mixed-basis" band structure program.

[1] J. C. Wooley, in *Compound Semiconductors,* edited by R. K. Willardson and H. L. Goering (Reinhold, New York, 1962), p. 3; A. N. Pikhtin, Fiz. Tekh. Poluprovodn. **11**, 425 (1971) [Sov. Phys. Semicond. **11**, 245 (1977)].

[2] S. Larach, R. E. Shrader, and C. F. Stocker, Phys. Rev. **108**, 587 (1957).

[3] A. A. El-Shazly, M. M. H. El-Naby, M. A. Kenawy, M. M. El-Nahass, H. T. El-Shair, and A. M. Ebrahim, Appl. Phys. A **36**, 51 (1985); R. Mach, P. Fl gel, L. G. Suslina, A. G. Areshkin, J. Maege, and G. Voigt, Phys. Status Solidi B **109**, 607 (1982).

[4] A. Ebina, M. Yamamoto, and T. Takahashi, Phys. Rev. B **6**, 3786 (1972).

[5] R. Hill and D. Richardson, J. Phys. C **6**, L115 (1973).

[6] J. A. Van Vechten and T. K. Bergstresser, Phys. Rev. B **1**, 3351 (1970).

[7] (a) A. Baldereschi, E. Hess, K. Maschke, H. Neumann, K. R. Schulze, and K. Unger, J. Phys. C **10**, 4709 (1977); (b) R. Hill and D. Richardson, *ibid.* **4**, L289 (1971); **4**, L339 (1971).

[8] (a) K. E. Newman and J. D. Dow, Phys. Rev. B **27**, 7495 (1983); (b) R. E. Allen, T. J. Humphreys, J. D. Dow, and O. F. Sankey, J. Vac. Sci. Technol. B **2**, 449 (1984).

[9] A. B. Chen and A. Sher, Phys. Rev. B **23**, 5360 (1981); **22**, 3886 (1980).

[10] J. C. Mikkelsen and J. B. Boyce, Phys. Rev. Lett. **49**, 1412 (1982).

[11] (a) W. E. Spicer, J. A. Silberman, J. Morgen, I. Lindau, J. A. Wilson, A. B. Chen, and A. Sher, Phys. Rev. Lett. **49**, 948 (1982); (b) K. E. Kirschfeld, N. Nelkowski, and T. S. Wagner, *ibid.* **29**, 66 (1972).

[12] A. Willig, B. Sapoval, K. Leibler, and C. Verie, J. Phys. C **9**, 1981 (1976).

[13] G. P. Srivastava, J. L. Martins, and A. Zunger, Phys. Rev. B **31**, 2561 (1985); A. Zunger and J. Jaffe, Phys. Rev. Lett. **51**, 662 (1983); J. L. Martins and Z. Zunger, *ibid.* **56**, 1400 (1986).

[14] T. S. Kuan, T. F. Kuech, W. I. Wang, and E. L. Wilkie, Phys. Rev. Lett. **54**, 201 (1985); H. R. Jen, M. J. Cherng, and G. B. Stringfellow, Appl. Phys. Lett. **48**, 1603 (1986).

[15] D. de Fontaine, in *Solid State Physics,* edited by H. Ehrenreich, F. Seitz, and D. Turnbull (Academic, New York, 1979), Vol. 34, p. 73.

[16] P. Bendt and A. Zunger, Phys. Rev. B **26**, 3114 (1982).

[17] J. L. Martins and A. Zunger, Phys. Rev. B **30**, 6217 (1984).

[18] P. N. Keating, Phys. Rev. **145**, 637 (1966).

[19] J. Jaffe and A. Zunger, Phys. Rev. B **29**, 1882 (1984).

[20] S. H. Wei and A. Zunger, Phys. Rev. Lett. **56**, 528 (1986).

[21] D. J. Chadi, Phys. Rev. B **16**, 790 (1977).

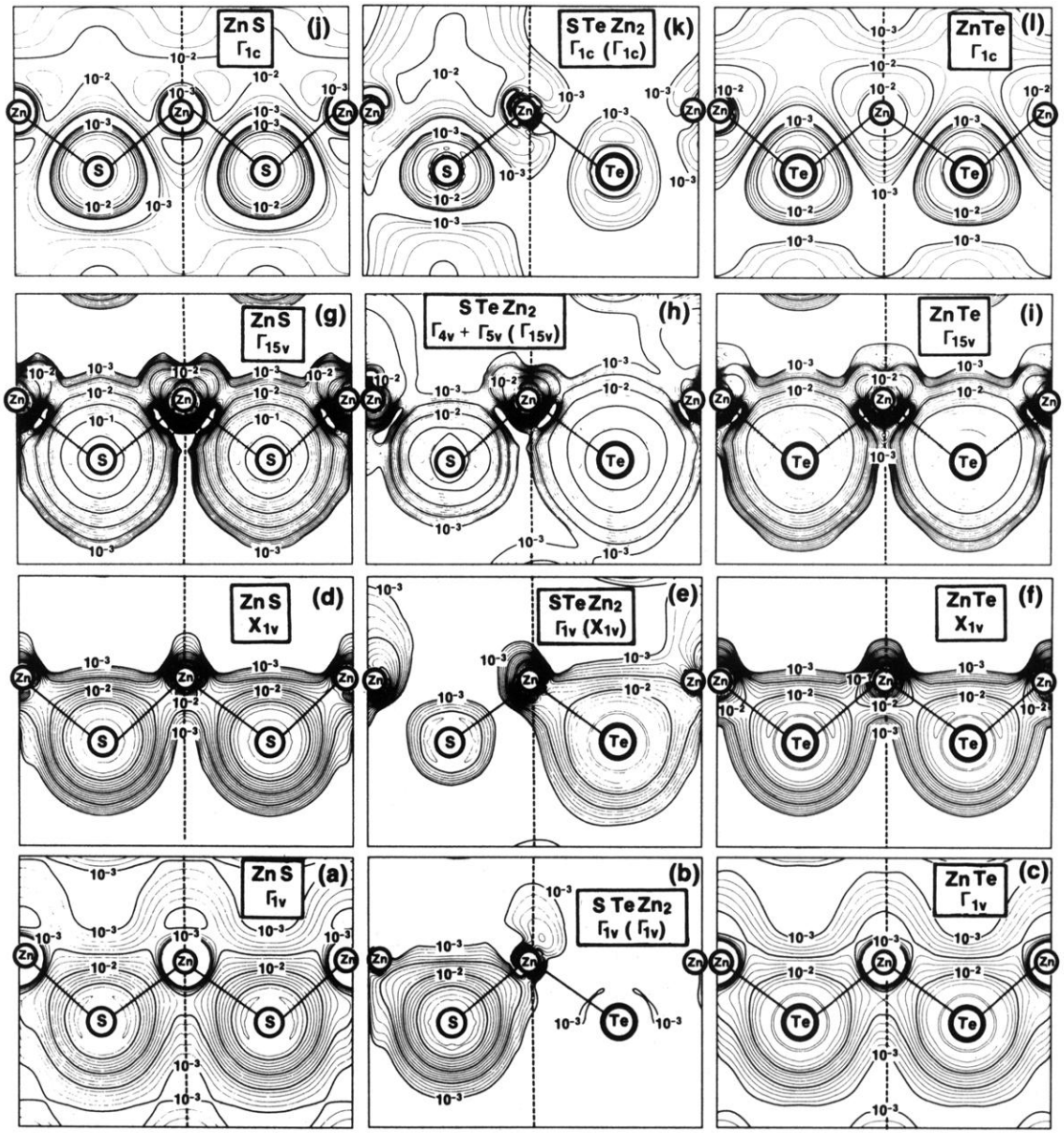

FIG. 1. Electronic charge-density contours (logarithmically spaced, in units of e/a.u.^{3}) of a few electronic states in ZnS (left), ZnTe (right), and their $STeZn_2$ alloy in the CuAu-I type structure (center). For the latter, we show both the band labels in $P\bar{4}m2$ symmetry and, in parentheses, the zinc-blende labels. Solid circles around atoms indicate core regions; straight solid lines denote bonds. The vertical dashed line is the symmetry plane for pure ZnS or ZnTe; this symmetry is broken in the alloy (central panels).